[CANCER RESEARCH 61, 2744–2750, March 15, 2001]

Sublethal Irradiation Promotes Migration and Invasiveness of Glioma Cells: Implications for Radiotherapy of Human Glioblastoma[1]

Christine Wild-Bode, Michael Weller, Andreas Rimner, Johannes Dichgans, and Wolfgang Wick[2]

Department of Neurology, Laboratory of Molecular Neuro-Oncology, University of Tübingen, Medical School, D-72076 Tübingen, Germany

ABSTRACT

Human malignant gliomas are highly lethal neoplasms. Involved-field radiotherapy is the most important therapeutic measure. Most relapses originate from the close vicinity of the irradiated target field. Here, we report that sublethal doses of irradiation enhance the migration and invasiveness of human malignant glioma cells. This hitherto unknown biological effect of irradiation is p53 independent, involves enhanced $\alpha_v\beta_3$ integrin expression, an altered profile of matrix metalloproteinase-2 and matrix metalloproteinase-9 (MMP-2 and MMP-9) expression and activity, altered membrane type 1 MMP and tissue inhibitor of metalloproteinases-2 expression, and an altered BCL-2/BAX rheostat favoring resistance to apoptosis. *BCL-2* gene transfer and irradiation cooperate to enhance migration and invasiveness in a synergistic manner. Sublethal irradiation of rat 9L glioma cells results in the formation of a greater number of tumor satellites in the rat brain *in vivo* concomitant with enhanced MMP-2 and reduced tissue inhibitor of metalloproteinases-2 expression. Collectively, these data suggest that the current concepts of involved-field radiotherapy for malignant glioma need to be reconsidered and that the pharmacological inhibition of migration and invasion during radiotherapy may represent a new therapeutic approach to improve the therapeutic efficacy of radiotherapy for malignant glioma.

INTRODUCTION

The median survival for human patients with glioblastoma, the most malignant form of glial tumor, is in the range of 1 year, even with aggressive multimodality treatment. Involved-field radiotherapy is the most important therapeutic measure and has been shown to prolong median survival for 6–8 months (1). However, up to 90% of all glioblastomas relapse in close proximity to the resection cavity or the target volume of postoperative radiotherapy (2–5). Only a small fraction of glioblastomas of 5–10% recur at a greater distance from the main tumor mass (6). This observation continues to foster strategies to enhance the local dose of irradiation applied to the presumptive tumor cell-bearing brain surrounding the tumor as defined by the contrast-enhancing lesion on cranial computed tomography or magnetic resonance imaging scans.

The integrin protein family represents the main cellular receptors for interactions with the extracellular matrix. Glioma cell motility on various substrates as well as penetration of membranes is mediated by integrins expressed on the cell surface of glioma cells. Similarly, activation of a vitronectin receptor, the $\alpha_V\beta_3$ integrin, is critical in anchorage-independent survival of small lung cancer cells (7). Constitutive and transforming growth factor-β-stimulated promotion of glioma cell migration is blocked by a monoclonal antibody to $\alpha_V\beta_3$ integrin or by the disintegrin, echistatin (8). Another vitronectin receptor, $\alpha_5\beta_1$ integrin, is required to internalize its ligand, vitronectin, and thus modulates the activity of $\alpha_V\beta_3$ (9). A mechanism to coordinate cellular migration and localization of proteolytic activity to discrete regions of the cell surface has been demonstrated for cultured melanoma cells. MMP-2 directly binds $\alpha_V\beta_3$ integrin and thus localizes in a proteolytically active form to the cell surface (10). The ability of glioma cells to spread on myelin depends on metalloproteolytic activity (11). The activation of wild-type p53 by irradiation and a resulting increase of MMP[3]-2 expression provide evidence for a scenario where irradiation might promote invasion-related gene expression (12). Successful migration and invasion of glioma cells require their resistance to the endogenous death program of apoptosis once the cell has detached from the bulk tumor. BCL-2, the prototype inhibitor of apoptosis, has been suggested to regulate cell-cell interactions (13), including integrin-dependent regulation of cell adhesion via r-ras (14). These data led to the discovery that ectopic BCL-2 expression promoted the motility of glioma cells *in vitro* (15). In the present study, we report that MMP, integrins, and BCL-2 family proteins cooperate to mediate an irradiation-induced increase in migratory and invasive glioma cell behavior. We provide a novel explanation for the local failure of radiotherapy: sublethal doses of irradiation promote the migration and invasiveness of glioma cells, which may then reach the border area of postoperative radiotherapy, escape delivery of a cumulatively lethal dose, and form the basis for locoregional relapse during or a few months after radiotherapy.

MATERIALS AND METHODS

Reagents and Cell Culture. The glioma cell lines used in this study have been described in previous studies (16, 17). NIH-3T3 murine fibroblasts cells were obtained from the American Type Culture Collection (Rockville, MD). Cells were cultured in DMEM supplemented with 10% FCS, 2 mM glutamine, and 1% penicillin/streptomycin and maintained at 37°C in an atmosphere of 5% CO_2. For acquisition of NIH-3T3-conditioned medium, the cells were grown in DMEM supplemented with 10% FCS, 2 mM glutamine, and 1% penicillin/streptomycin to subconfluent monolayers, washed with PBS, and then incubated with serum-free DMEM for 48 h. Supernatant was harvested and stored at −20°C. Echistatin and *o*-phenantroline were obtained from Sigma (Deisenhofen, Germany).

Irradiation. Cells were grown to 70% confluence in DMEM and trypsinized or grown to spheroids as detailed and irradiated in a Gammacell 1000 (^{137}Cs; Nordion, Kanata, Ontario, Canada) at 1–8 Gy. Clonogenic cell death was assessed in six-well plates at a seeding density of 500 cells/well. The cells were irradiated and further cultured for 3 weeks. The culture dishes were stained with crystal violet. Colonies of >50 cells were counted at low magnification.

Immunoblot Analysis. For the preparation of whole-cell lysates, the cells were rinsed in PBS, harvested, centrifuged at 1200 × *g*, lysed in 0.1 M Tris-HCl (pH 7.2) containing 0.1% NP40, 0.1 mM EDTA, and 5 μg/ml phenylmethylsulfonyl chloride for 40 min on ice, and centrifuged at 10,000 × *g* for 10 min. Protein concentration was assayed using Bio-Rad reagents with photometric analysis. For the preparation of soluble supernatant protein, the protein concentration of supernatant was determined, and 20 μg of soluble supernatant protein were precipitated with acetone at −20°C for 12 h and pelleted at 10,000 × *g* for 10 min. Twenty μg of protein/lane were separated by 10–15% SDS-PAGE and electroblotted on nitrocellulose (Amersham, Braunschweig, Germany). Equal protein loading was ascertained by

Received 9/15/00; accepted 1/17/01.

The costs of publication of this article were defrayed in part by the payment of page charges. This article must therefore be hereby marked *advertisement* in accordance with 18 U.S.C. Section 1734 solely to indicate this fact.

[1] Supported by the Interdisciplinary Center of Clinical Research Tübingen (to W. W.) and the Wilhelm Sander-Foundation (to W. W. and M. W.).

[2] To whom requests for reprints should be addressed, at Department of Neurology, University of Tübingen, School of Medicine, Hoppe-Seyler-Strasse 3, 72076 Tübingen, Germany. Phone: 49-7071-298-2141; Fax: 49-7071-29-5260; E-mail: wolfgang.wick@uni-tuebingen.de.

[3] The abbreviations used are: MMP, matrix metalloproteinase; MT-1-MMP, membrane type 1 MMP; TIMP, tissue inhibitor of metalloproteinases.

Ponceau S staining. After blocking for 1 h in PBS supplemented with 5% skim milk and 0.1% Tween 20, immunodetection of MMP-2 (M_r 72,000)/MMP-9 (M_r 92,000), TIMP-2 (M_r 21,000), MT-1-MMP (M_r 66,000) (2 μg/ml; Oncogene, Calbiochem, Schwalbach, Germany), BCL-2 (M_r 26,000), BCL-X_L (M_r 27,000), BAX (M_r 21,000), and TP53 (M_r 53,000) was performed using rabbit polyclonal antibodies (2 μg/ml; Santa Cruz Biotechnology, Santa Cruz, CA). Antirabbit or antimouse IgG (1:4000; Santa Cruz Biotechnology) and enhanced chemiluminescence (ECL; Amersham) were used for detection.

Zymography. MMP-2 and MMP-9 activity were analyzed as detailed elsewhere (15). Briefly, 20 μg of soluble supernatant protein were separated by 10% SDS-PAGE containing 0.1% gelatin without denaturing agents. Gels were washed twice for 30 min in 50 mM Tris-HCl (pH 7.5) and 2.5% Triton X-100 and then incubated overnight at 37°C in 50 mM Tris-HCl (pH 7.6), 10 mM $CaCl_2$, 150 mM NaCl, and 0.05% NaN_3 to allow the gelatinases to digest the gelatin structure. Gels were stained with Coomassie Brilliant Blue R-250 and then destained with 90% methanol:H_2O (1:1) and 10% glacial acetic acid. Because of gelatinolytic activity, bright bands are visible at M_r 92,000 for MMP-9 and M_r 72,000 for MMP-2.

Flow Cytometry. For $\alpha_v\beta_3$ and $\alpha_5\beta_1$ integrin analysis, the glioma cells were treated as indicated, washed with PBS, incubated with trypsin for 30 s at room temperature and harvested. Five $\times$ 10^5 cells were incubated with 1 μg each of $\alpha_v\beta_3$ integrin or $\alpha_5\beta_1$ integrin mouse monoclonal antibody (Chemicon, Hofheim, Germany) or 1 μg of mouse IgG isotype control antibody (Sigma, Deisenhofen, Germany) in 100 μl of PBS/0.1% BSA for 30 min at 4°C protected from light. The cells were washed twice with PBS and analyzed on a FACScalibur flow cytometer using Cell Quest acquisition and analysis software (Becton Dickinson, Heidelberg, Germany).

Northern Blot Analysis. Total RNA was isolated using the RNeasy RNA purification system (Qiagen, Hilden, Germany). RNA (10 μg) was electrophoresed and transferred on a nylon membrane (Hybond N; Amersham, Braunschweig, Germany). Equal mRNA loading was assured by methylene blue staining. The membrane was cohybridized to ^{32}P-labeled α_v and β_3 cDNA probes. For the generation of cDNA probes, 5 μg of total RNA extracted from LN-18 cells were subjected to reverse transcription using SuperScript II (Life Technologies, Inc., Gaithersburg, MD) and oligo(dT) priming (Amersham Pharmacia Biotech, Uppsala, Sweden). Integrin α_v and β_3 cDNA fragments were PCR amplified using primers TTCAACCTAGACGTGGA-CAG (nucleotides 132–152) and GATCTACATGGAGCATACTC (nucleotides 543–562) for integrin α_v and GTGACCTGAAGGAGAATCTG (nucleotides 207–226) and TATGGTGACAC-AGGCTTGTC (nucleotides 566–585) for integrin β_3. Purified cDNA fragments (20 ng) were labeled with [^{32}P]dCTP (Amersham Pharmacia Biotech) using Rediprime II random prime labeling system (Amersham Pharmacia Biotech). After hybridization, the filters were washed, and bound radioactivity was assayed on a phosphorimager using TINA analysis software (Fuji BasReader 1500; Raytest, Staubenhardt, Germany).

Migration Assay. Migration of malignant glioma cells through 8-μm pores was assessed using a 48-well micro chemotaxis chamber (Neuro Probe, Inc., Bethesda, MD). NIH-3T3-conditioned medium (30 μl) was pipetted as a chemoattractant into the lower wells. The filter membrane was placed between the top and bottom chambers and equilibrated for 30 min at 37°C. Two $\times$ 10^4 cells in medium alone or medium containing *o*-phenantroline (100 μM) or $\alpha_v\beta_3$ integrin antibody with blocking action (10 μg/ml) or mouse IgG isotype control antibody (10 μg/ml) were applied to the upper wells and allowed to migrate through the membrane at 37°C in humidified air with 5% CO_2. After 24 h, the membrane was removed, and the nonmigrated cells were removed with a wiper blade. Migrated cells on the bottom side of the membrane were fixed in methanol and then stained in thiazine and eosin solution using DiffQuick (Dade Behring AG, Düdingen, Switzerland). Quantification was done by counting five fields at 20 $\times$ magnification with a microscope. Cells were counted twice by two independent investigators (C. W. B. and W. W.). Interobserver variation was <5%.

Matrigel Invasion Assay. Invasion of glioma cells *in vitro* was measured by the invasion of cells through Matrigel-coated transwell inserts (Becton Dickinson; Ref. 18). Briefly, transwell inserts with 8-μm pore size were coated with Matrigel (0.78 mg/ml). Cells were trypsinized, and 200 μl of cell suspension (3 $\times$ 10^5 cells/ml) per condition were added in triplicate wells. 3T3-conditioned medium (500 μl) was added to the lower well. Cells on the lower side of the membrane were fixed, stained in thiazine and eosin solution using DiffQuick (Dade Behring AG), and sealed on slides. Quantification of invasion through the coated membranes was done by counting stained cells using a microgrid. Cells were counted twice by two independent investigators (C. W. B. and W. W.). Interobserver variation was <5%.

Glioma Spheroids. Multicellular glioma spheroids were cultured in 25-cm^2 culture flasks base-coated with 0.75% Noble Agar (Difco Laboratories, Detroit, MI) prepared in DMEM (19). Briefly, 3 $\times$ 10^6 cells were suspended in 10 ml of medium, seeded onto 0.75% agar plates, and cultured until spheroids had formed. Spheroids of ~200-μm diameter were selected for the experiments. The area covered by glioma cells migrating from a tumor spheroid explanted on a plastic surface was used as an index of cell migration. Spheroids were transferred individually to 96-well plates containing 200 μl of serum-free medium. Every 24 h for 4 days, the radial distance of migration was determined after subtraction of the initial spheroid diameter at time zero from the diameter of the area covered with cells migrated from the spheroid.

Fetal Rat Brain Aggregates. Fetal rat brain aggregates were obtained from 18-day-old fetuses of BD9 rats. The brains were aseptically removed and placed into a sterile tissue culture plate containing PBS. The brain tissue was minced, washed in PBS, and dissociated by serial trypsinization. Single-cell suspensions were obtained and plated into agar-coated, 24-well plates at an average of the cell amount of one brain/well in 2 ml of medium. After 48 h, aggregates were transferred to new plates and cultured for 19 days. Aggregates with ~200-μm diameter were used in additional experiments (19).

Confrontation Assays. Invasion of the glioma spheroids into fetal brain aggregates was analyzed by morphometry using the MCID digitalization system (Imaging Research, Inc., Ontario, Canada). Briefly, tumor spheroids and rat brain aggregates were transferred in triplicate to individual wells of a 96-well plate, base-coated with agar. With the help of a sterile syringe and a microscope, tumor spheroids and fetal brain aggregates were placed in close contact to each other. Images were obtained at 24-h intervals.

***In Vivo* Studies.** Fisher rats (Charles River, Sulzfeld, Germany) were housed in groups of three or four under standard conditions at a temperature of 22°C and a 12-h light-dark cycle. They had free access to standard food pellets and tap water. For surgery, 12-week-old male rats weighing 180–200 g were anesthetized with Previmytal (500 mg in 10 ml of NaCl 0.9%), and 10,000 logarithmic-phase 9L cells were injected stereotactically into the striatum. In the first group, adherent cells were irradiated at 1 or 3 Gy, dissociated with cell dissociation buffer, and dissolved in PBS prior to implantation. In the second group, cells were treated accordingly but not irradiated. At 21 days, the rats were sacrificed. The brains were shock frozen in liquid nitrogen and cut in 8-μm sections for histology or 20-μm sections for volumetry. Thirty sections/tumor were analyzed for volumetry. Tumor volumes were determined on H&E-stained sections with the MCID digitalization system (Imaging Research, Inc.). For determination of invasiveness, brain sections were stained with a nestin antibody (20) that specifically stains the 9L tumor cells, not surrounding brain, according to a standard protocol. Briefly, slides were incubated with acetone for 10 min, air dried, incubated with 1% H_2O_2 for 30 min, washed with PBS, and blocked with BSA (10 mg/10 ml PBS) for 10 min. Nestin antibody (1:1000; PharMingen, Hamburg, Germany) was added overnight. Bound primary antibody was labeled with biotinylated antimouse IgG antibodies, washed, incubated with avidin-biotin reagent (Vectastain Elite ABC peroxidase; Vector, Wiesbaden, Germany), and developed in diaminobenzidine (Sigma). As a control, the first antibodies were replaced by whole preimmune serum. Because the margins of 9L tumors are characterized by the lack of an infiltration zone, unlike human gliomas, the bulk tumor mass is easily recognized. This is true for H&E sections but also for nestin immunochemistry, because the glioma cells, but not the parenchymal brain cells, expressed nestin. Nestin-positive tumor cell clusters (with clusters being defined as tumor cell aggregates >10 cells) distant from the bulk tumor mass were counted on six independent 8-μm sections/tumor.

Statistical Analysis. Quantitative data were obtained for migration, invasion, $\alpha_V\beta_3$ mRNA expression and protein levels, tumor volumes, and tumor cell satellite counts as indicated above. The experiments were usually performed in triplicate and repeated three times. The significance of the observed effects was evaluated by *t* test at $P < 0.05$ and $P < 0.01$. Synergy was determined by the fractional product method (21).

RESULTS

Irradiation Promotes Glioma Cell Migration: Reversal by an Inhibitor of $\alpha_V\beta_3$ Integrin. The radiosensitivity of U87 MG, LN-18, and LN-229 cells was examined in a conventional colony formation assay (Fig. 1*A*). Enhanced migration and invasion of irradiated glioma cells became apparent at 24 h after irradiation, in a dose-dependent manner, both at sublethal doses and at doses that significantly reduce clonogenic survival in all three cell lines (Fig. 1, *B–E*).

The effects of irradiation on migration and invasion were a priori unlikely to depend on p53 because LN-18 cells do not retain functional p53 activity. To confirm this, we took advantage of U87 MG or LN-229 cells engineered to express the dominant-negative p53 mutant $p53^{V143A}$ (22). As reported previously, the $p53^{V143A}$-expressing cells, in contrast to control cells, did not accumulate p21 in response to genotoxic stress. p21 accumulation is a classical p53-mediated response, and its suppression confirms the abrogation of wild-type p53 function (23). However, ectopic expression of $p53^{V143A}$ in U87 MG and LN-229 cells did not result in an altered response to irradiation as concerns migration or invasion (data not shown).

Next, we analyzed the requirement for integrins in the irradiation-induced migratory phenotype. The expression of mRNA and protein of $\alpha_V\beta_3$ integrin was enhanced by irradiation in all three cell lines (Fig. 2, *A–D*). Expression of $\alpha_V\beta_3$ integrin was similarly enhanced in the $p53^{V143A}$-expressing U87 MG cells and the control-transfected p53 wild-type U87 MG cells (Fig. 2*D*). In contrast, the expression of $\alpha_5\beta_1$ integrin was not modulated by irradiation (Fig. 2*E*). Echistatin, an inhibitor of $\alpha_V\beta_3$ and $\alpha_5\beta_1$ integrins (24), abrogated constitutive and irradiation-enhanced migration and invasion (data not shown). A specific anti-$\alpha_V\beta_3$ integrin antibody (10 μg/ml) inhibited baseline migration and almost abrogated the promotion of migration by irradiation at 1 and 3 Gy (Fig. 2*F*). These data indicate that $\alpha_v\beta_3$ integrin is involved in irradiation-promoted cell motility but also show that the role for integrins in migration is not specific for irradiation-enhanced migration. This is because echistatin and the $\alpha_V\beta_3$ antibody prevented both constitutive and irradiation-enhanced migration.

Irradiation Alters MMP Expression and Activity. Because MMP activity is thought to be required for glioma cell migration and invasion, we next asked whether irradiation altered MMP expression

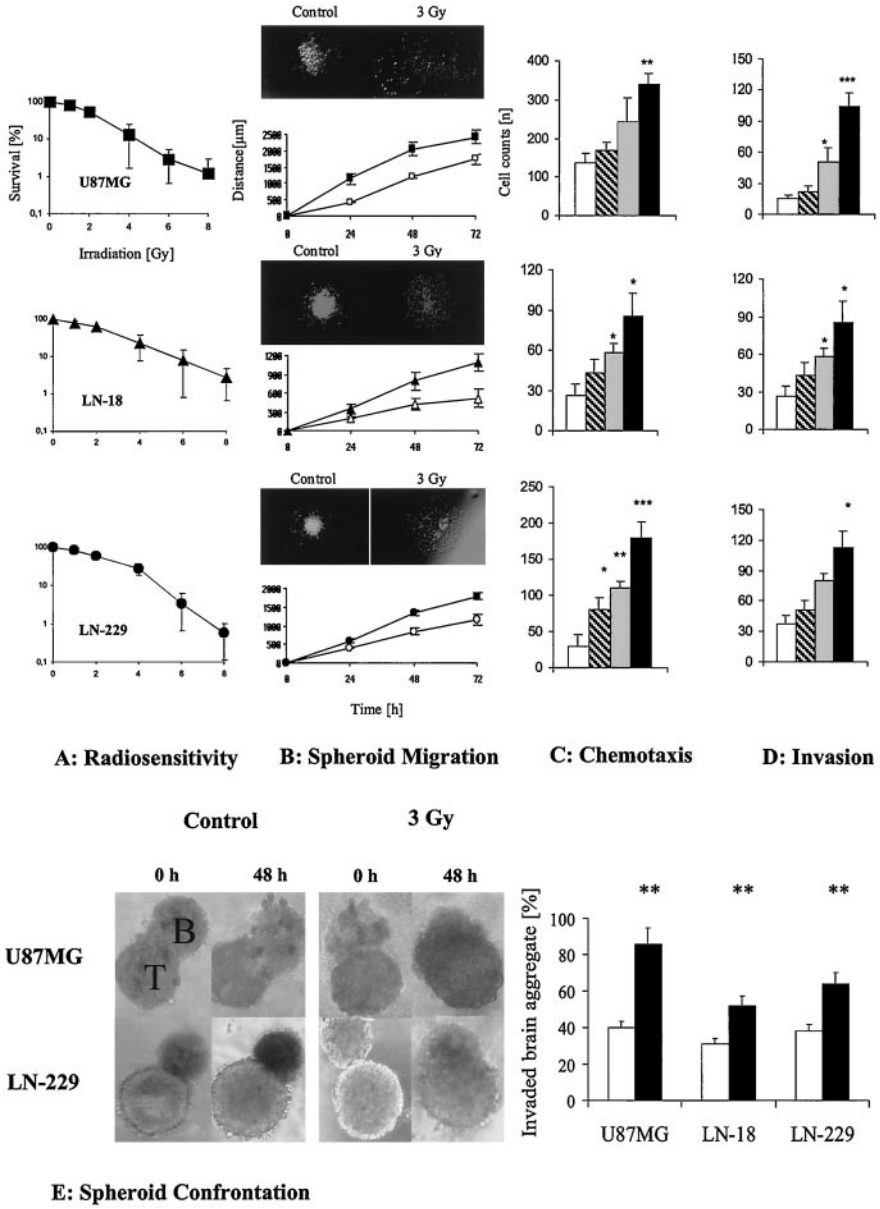

Fig. 1. Sublethal irradiation promotes glioma cell migration *in vitro*. *A*, U87 MG, LN-18, or LN-229 cells were irradiated as indicated. Clonogenic survival was assessed 3 weeks later as described in "Materials and Methods." *B*, tumor cell spheroids derived from U87 MG, LN-18, or LN-229 were prepared and seeded. The spheroids were untreated (*open symbols, left*) or irradiated at 3 Gy (*closed symbols, right*). The median distance in μm from the center of the spheroid minus the diameter of the spheroid was measured for 50 migrated cells at 24, 48, and 72 h. Data are expressed as means of three independent experiments performed in triplicate; *bars*, SE. *C*, chemotaxis assays were performed with 2×10^4 cells that were untreated (□) or irradiated at 1 Gy (▨), 3 Gy (▨), or 6 Gy (■). Migrated cells were counted at 24 h as indicated in "Materials and Methods." *D*, glioma cell invasion was assessed at 24 h after irradiation with 0 (□), 1 Gy (▨), 3 Gy (gray bar), or 6 Gy (■) in a Boyden chamber assay. Data are expressed as mean cell counts ($n = 3$); *bars*, SE. *, $P < 0.05$; **, $P < 0.01$; ***, $P < 0.001$. *E*, the confrontation experiments were done as documented in "Materials and Methods." The images (*top panel*, U87 MG untreated at 0 and 48 h or treated with 3 Gy at 0 and 48 h; *bottom panel*, LN-229 untreated at 0 and 48 h or treated with 3 Gy at 0 and 48 h) show the brain aggregate (*B*) smaller and the tumor spheroid (*T*) relatively larger. Quantification was done by assessing the area of the invaded brain aggregate relative to the original size in a percentage. Confrontation experiments with untreated control spheroids (□) or spheroids irradiated at 3 Gy (■) were performed three times in triplicate; **, $P < 0.01$.

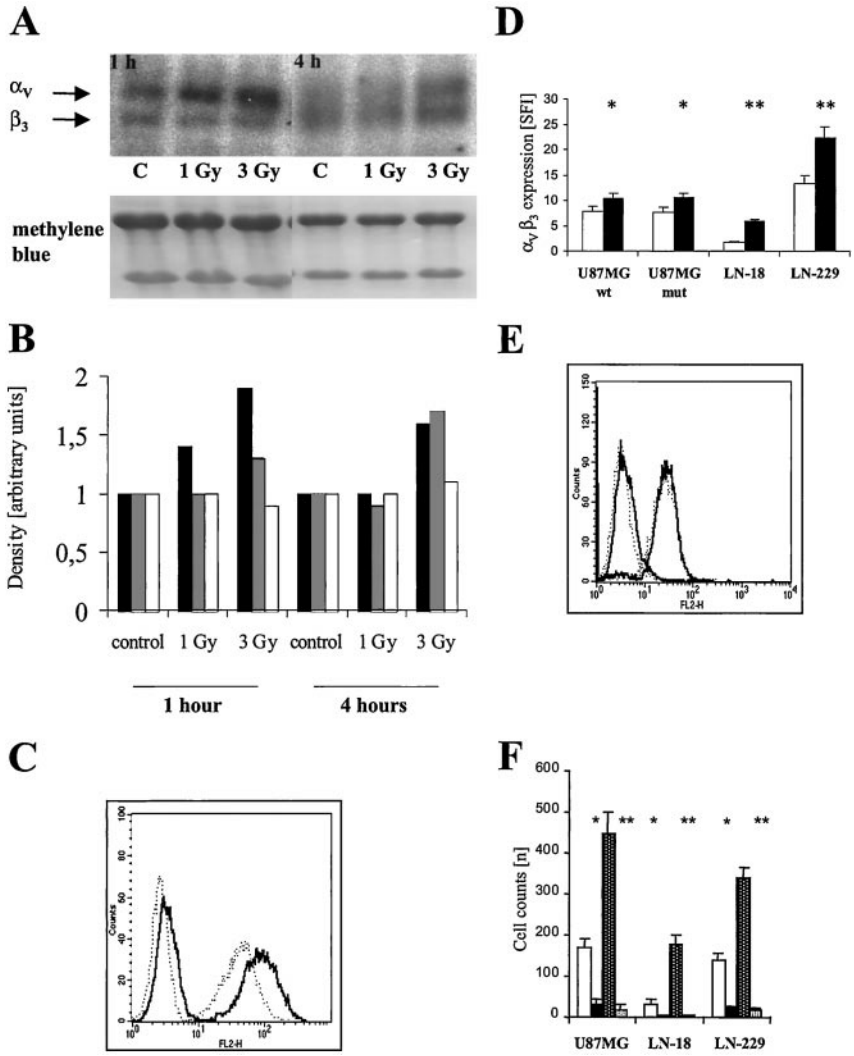

Fig. 2. Irradiation enhances $\alpha_V\beta_3$ integrin expression. *A*, Northern blot analysis for α_V (7.5 kb) and β_3 mRNA expression (6 kb) was performed on RNA obtained from untreated cells or cells irradiated at 1 or 3 Gy after 1 or 4 h. Equal mRNA loading was ascertained by methylene blue staining. *B*, quantification was done with standard software as documented in "Materials and Methods." Controls for α_V (■), β_3 (▨), and methylene blue (□) were set 1.0. Irradiated bands were normalized to untreated controls and loading control (methylene blue). *C*, LN-229 cells were untreated or irradiated at 3 Gy. $\alpha_V\beta_3$ integrin expression was assessed by flow cytometry. *Bold profiles*, isotype control and specific $\alpha_v\beta_3$ integrin antibody in irradiated cells; *thin lines*, nonirradiated cells. *D*, U87 MG p53-wild type or p53-mutant, LN-18, and LN-229 cells were untreated (□) or irradiated at 6 Gy (■). Data are expressed as mean specific fluorescence index (SFI); *bars*, SE ($n = 3$). *, $P < 0.05$, *t* test. *E*, LN-229 cells were untreated or irradiated at 3 Gy. $\alpha_5\beta_1$ integrin expression was assessed by flow cytometry. *Bold profiles*, isotype control and specific $\alpha_5\beta_1$ integrin antibody in irradiated cells; *thin lines*, nonirradiated cells. *F*, migration experiments as in Fig. 1*C* were performed in irradiated glioma cells that were allowed to migrate for 24 h in the presence of an $\alpha_v\beta_3$ integrin antibody with blocking action (10 μg/ml) or in the presence of a control mouse IgG antibody (10 μg/ml). □, cells treated with mouse IgG control antibody; ■, $\alpha_v\beta_3$ integrin antibody-treated cells; ▨, cells irradiated at 3 Gy and treated with mouse IgG isotype control antibody; ▧, cells irradiated at 3 Gy and treated with $\alpha_v\beta_3$ integrin antibody. Data are expressed as mean cell counts; *bars*, SE ($n = 3$). *, $P < 0.05$; **, $P < 0.01$ (*t* test, compared with nonirradiated cells in the presence of a mouse IgG isotype control antibody).

and activity. Immunoblot analysis revealed an increase of MMP-2 expression in response to irradiation in U87 MG cells but not in LN-18 or LN-229 cells (Fig. 3*A*). However, zymography showed that MMP-2 activity was elevated after irradiation in all three cell lines. Also, activation of MMP-9 was dramatically enhanced in irradiated U87 MG and became only detectable after irradiation in the other two cell lines. Furthermore, the levels of MT-1-MMP were markedly enhanced in irradiated glioma cells. Conversely, the levels of TIMP-2 were strongly reduced in all cell lines. Consistent with our findings in the motility assays and the flow cytometric analysis of $\alpha_V\beta_3$ integrin levels, the ectopic expression of the dominant-negative $p53^{V143A}$ did not alter the irradiation-induced increase in metalloproteinase expression and activity in U87 MG cells (data not shown). Consistent with an important role of MMP activity in constitutive and irradiation-enhanced invasion, pretreatment with 100 μM of the MMP inhibitor, *o*-phenantroline, significantly reduced invasion under all experimental conditions, whereas a concentration of 25 μM abolished only the radiation-induced enhancement (Fig. 3*B*). Furthermore, pretreatment of LN-229 cells with 25 μM *o*-phenantroline abolished the radiation-induced MMP-2 and MMP-9 activation (Fig. 3*C*). To exclude an interaction between the inhibitory effect of *o*-phenantroline on migration and clonogenic cell death induced by irradiation, we showed that *o*-phenantroline at 100 μM did not modulate clonogenic cell death after irradiation at 1 or 3 Gy in either cell line (data not shown).

Irradiation Modulates BCL-2 Family Protein Expression. We have reported previously that ectopic expression of a *BCL-2* transgene promotes migration and invasiveness in human glioma cells (15). Consequently, we assessed a possible modulation of BCL-2 family protein expression by irradiation. Fig. 4*A* shows that the levels of the antiapoptotic BCL-2 and BCL-X_L proteins increased in response to irradiation in all three cell lines. Ectopic expression of dominant-negative $p53^{V143A}$ in U87 MG cells did not alter the irradiation-induced change in BCL-2 levels (Fig. 4*A*). In contrast, the levels of the proapoptotic BAX protein were slightly reduced in U87 MG cells but unaffected by irradiation in the other cell lines. Thus, irradiation induced cell line-specific changes in the patterns of BCL-2 family protein expression that consistently resulted in a more apoptosis-resistant phenotype. Consistent with our previous observations that exogenous BCL-2 expression in glioma cells leads to an invasive phenotype via up-regulation of metalloproteolytic activity (15), we did not detect any alteration in expression levels of BCL-2, BCL-X_L, or BAX when the cells were pretreated with *o*-phenantroline (data not shown), indicating that changes in BCL-2 family protein expression are upstream of MMP activation in this paradigm. In addition, this shows that modification of the BCL-2:BAX ratio itself is not sufficient to support cell motility because *o*-phenantroline stops cell invasion.

To further evaluate the interrelations between the irradiation effects

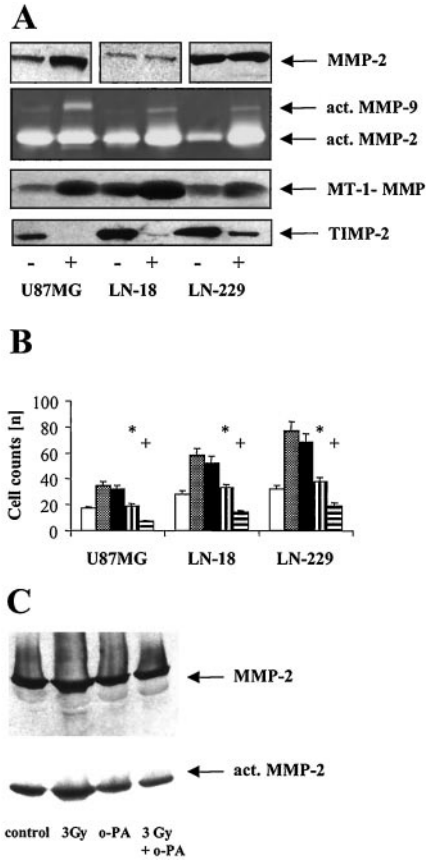

Fig. 3. Irradiation enhances MMP expression and activity. *A*, soluble lysates from untreated or irradiated cells were prepared at 24 h after irradiation (3 Gy) and analyzed for MMP-2 levels by immunoblot analysis. Supernatants from untreated or irradiated cells were collected 24 h after irradiation (3 Gy), concentrated, and analyzed for active MMP-2 and MMP-9 by zymography as detailed in "Materials and Methods" (activity of MMP-2/MMP-9). Lysates from untreated or irradiated (3 Gy) were assessed for MT-1-MMP and TIMP-2 levels. *B*, invasion experiments as in Fig. 1*D* were performed in glioma cells irradiated at 3 Gy that were either untreated or cotreated for 24 h during invasion with *o*-phenantroline (10, 25, or 100 μM). □, untreated control cells; ▩, cells irradiated at 3 Gy; ■, cells irradiated at 3 Gy and treated with 10 μM *o*-phenantroline; ▥, cells irradiated at 3 Gy and treated with 25 μM *o*-phenantroline; ▤, cells treated with 100 μM *o*-phenantroline only. Data are expressed as mean cell counts ($n = 3$); *bars*, SE. *, $P < 0.05$, compared with irradiated cells in the absence of *o*-phenantroline; +, $P < 0.05$, compared with nonirradiated cells in the absence of *o*-phenantroline. *C*, immunoblot and zymography for MMP-2 were done as in *A* with untreated LN-229 control cells (*Lane 1*), cells irradiated at 3 Gy (*Lane 2*), cells treated with 25 μM *o*-phenantroline (*o-PA*) only (*Lane 3*), and cells irradiated at 3 Gy and treated with 25 μM *o*-phenantroline (*Lane 4*). *act.*, activated.

and BCL-2 family proteins, we examined the response of *BCL-2*-transfected cells (15) to irradiation. Glioma cells engineered to express a murine *BCL-2* transgene also responded to irradiation with enhanced migration and invasiveness (Fig. 4*B*). According to the fractional product method, the effects of irradiation and *BCL-2* gene transfer on migration and invasion were synergistic in LN-18 and in LN-229 cells (*e.g.*, additive effect: expected for invasion of irradiated LN-18 would be $1.9 \times 22 = 41.8$, but the value actually observed, 49, is synergistic). Note that the survival-promoting properties of BCL-2 do not influence the data reported in Fig. 4 because irradiation at these doses does not induce any cell loss within the time frame of these experiments (data not shown).

Irradiation Promotes Glioma Cell Dissemination *in Vivo*. The observed promigratory and proinvasive effect of sublethal irradiation in human glioma cell lines may have great clinical relevance. We therefore chose the intracerebral rat 9L glioma model to examine the growth pattern of preirradiated 9L glioma cells *in vivo*. To this end, 9L cells were irradiated and implanted into the basal ganglia 30 min later. Three weeks after implantation, histological analysis revealed that the tumors formed by irradiated cells were more invasive and exhibited multiple tumor cell satellites in the periphery of the bulk tumor (Fig. 5*A*). The tumor sizes did not differ significantly between irradiated and control cells (Fig. 5*B*). Nestin immunochemistry was found to be a suitable marker to detect glioma cell spreading in the 9L glioma model (Fig. 6). The intermediate filament nestin has been found to be reexpressed in primary central nervous system tumors but not in adult brain (20). Similarly, the brain of adult Fisher rats in contrast to implanted 9L tumor cells does not show immunoreactivity for nestin (25). Consistent with the *in vitro* data (Fig. 3), tumors formed by irradiated cells showed stronger MMP-2 expression than control tumors, whereas TIMP-2 was reduced (Fig. 6).

DISCUSSION

Involved-field radiotherapy has remained the single most effective treatment of glioblastoma for >20 years. Dose escalations beyond 60 Gy have resulted in unacceptable toxicity to the brain, *e.g.*, local necrosis or serious leukencephalopathy. Because glioblastoma cells are highly migratory and invasive tumor cells and because relapses were commonly observed in the vicinity of the initial tumor manifestation but not in the center of the target volume for radiotherapy, expanding the target volume of irradiation to the whole brain has been examined for neurotoxicity and therapeutic efficacy (3, 5). Whole brain irradiation has not decreased the risk of recurrence or altered the site of recurrent tumor but has seriously increased the risk of neuropsychological deficits, *e.g.*, dementia (4). Brachytherapy, *i.e.*, ster-

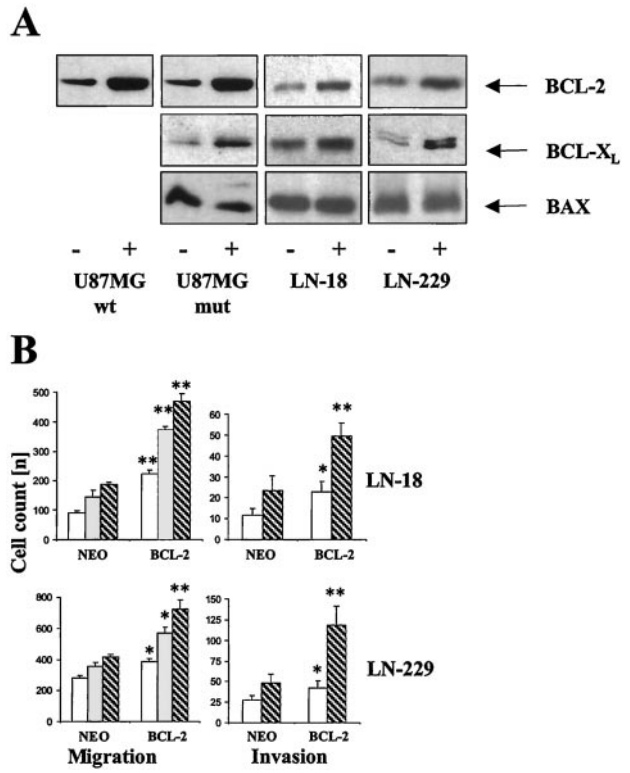

Fig. 4. Irradiation alters BCL-2 family protein expression in favor of an apoptosis-resistant phenotype. *A*, U87 MG p53-wild type or p53-mutant, LN-18, or LN-229 cells were untreated (−) or irradiated with 3 Gy (+). Soluble protein lysates were prepared 24 h later and analyzed for BCL-2, BCL-X_L, or BAX content by immunoblot analysis. *B*, NEO control transfectants or BCL-2-transfected sublines were untreated (□) or irradiated with 1 Gy (*gray bars*) or 3 Gy (▧) and then assessed for migration and invasiveness as in Fig. 1, *C* and *D*. Data are expressed as mean cell counts ($n = 3$); *bars*, SE. *, $P < 0.05$; **, $P < 0.01$ (compared with control-transfected cells). Synergy was determined according to the fractional product method.

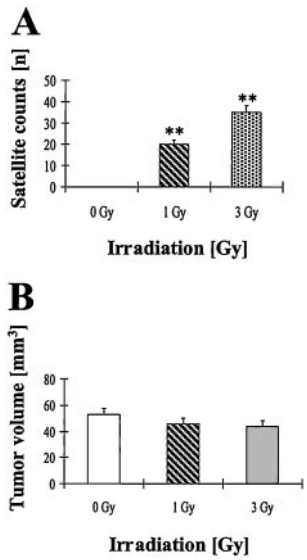

Fig. 5. Irradiation enhances 9L rat glioma cell dissemination *in vivo*. 9L rat glioma cells were untreated or irradiated with 1 or 3 Gy and implanted stereotactically into the striatum of Fisher rats as detailed in "Materials and Methods." *A*, at 21 days brains were fixed, cut, and stained with nestin (see also Fig. 6, *top panel*), and tumor cell satellites consisting of >10 cells in one cluster distant from the main tumor mass were counted. *Bars*, SE. **, $P < 0.01$, compared to nonirradiated cells. *B*, tumor volumes of H&E-stained brains were determined with the MCID digitalization system. *Bars*, SE. Data are expressed as mean satellite counts and SEM ($n = 6$).

eotactic interstitial irradiation using temporary high activity isotopes, is used as an alternative to conventional radiotherapy with the aim to provide a high dose of irradiation to the targeted volume, thereby potentially enhancing local control, with minimal toxicity to healthy tissue surrounding the tumor bed. Interestingly, this therapeutic modality has led to a significant increase in recurrencies at distant sites (3, 26). This effect of brachytherapy has usually been attributed to implantation-induced spread and contamination of unaffected brain tissue. Although this remains a possible explanation for the increased frequency of distant recurrence in patients treated with brachytherapy, the effects of sublethal doses of irradiation on migration and invasion reported here (Figs. 1, 5, and 6) suggest that ionizing irradiation from the implanted isotope might promote centrifugal migration and invasion of cells at the tumor brain border.

Enhanced migration and invasiveness of sublethally irradiated glioma cells involved enhanced $\alpha_V\beta_3$ but not $\alpha_5\beta_1$ integrin expression (Fig. 2), enhanced MMP activity (Fig. 3), and changes in BCL-2 family protein expression toward an apoptosis-resistant phenotype (Fig. 4*A*). Parallel studies using isogenic U87 MG and LN-229 sublines expressing the dominant-negative $p53^{V143A}$ mutant revealed that p53 does not mediate these changes induced by irradiation (Figs. 2*D* and 4*A*, and data not shown). Regulation of BCL-2 by irradiation is necessary to be upstream of metalloprotease regulation because the metalloprotease inhibitor *o*-phenantroline reduced metalloprotease activation without affecting BCL-2 expression (Fig. 3). The changes in integrin expression and MMP activity were both required for the effect of irradiation because echistatin and an $\alpha_V\beta_3$ integrin antibody as well as *o*-phenantroline abrogated the irradiation-induced increase in migration and invasiveness (Figs. 2 and 3). However, this is dose dependent. Low concentration of both echistatin and *o*-phenantroline abolish the radiation-induced effect but higher concentrations also inhibit baseline migration and invasion. The irradiation-induced changes in BCL-2 family protein expression would be predicted to confer a survival advantage in the face of subsequent postirradiation

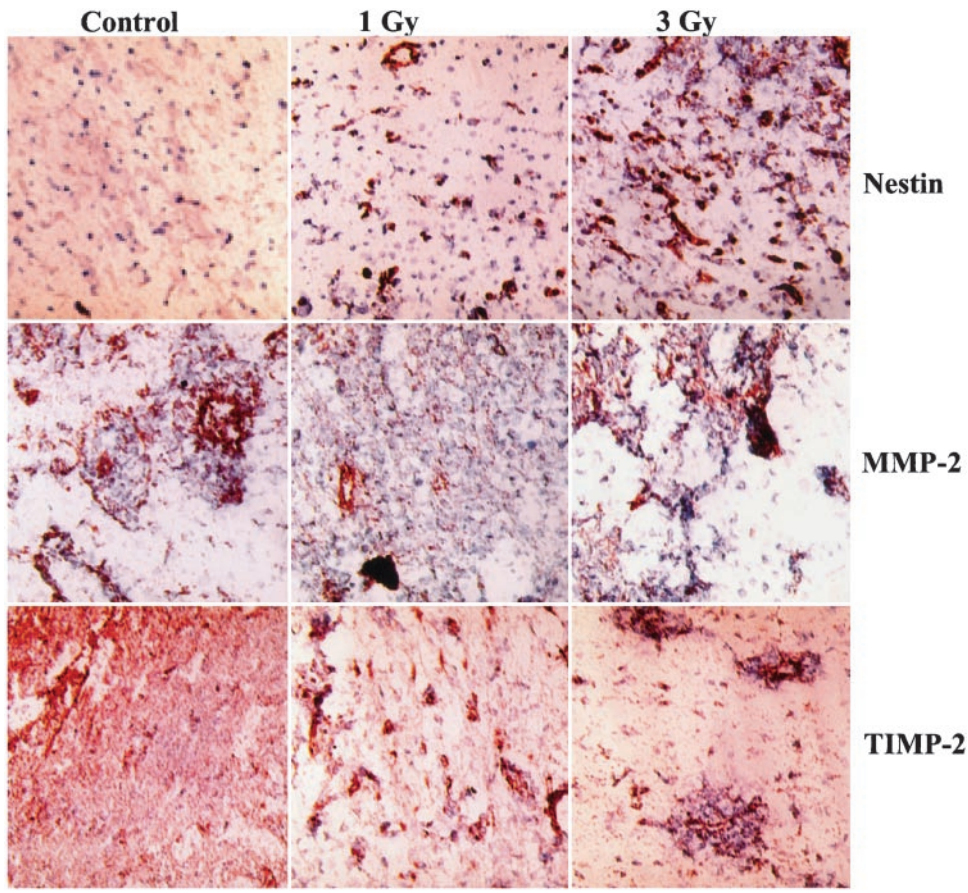

Fig. 6. Irradiation promotes MMP expression and activity *in vivo*. 9L gliomas generated from control cells or irradiated cells were analyzed for nestin, MMP-2, or TIMP-2 immunoreactivity as outlined in "Materials and Methods." ×200.

chemotherapy (27). Moreover, our previous clinicopathological correlative studies have identified a shift toward antiapoptotic BCL-2 family protein expression in human gliomas progressing or relapsing after radiochemotherapy (28). Finally, irradiation induced a promigratory profile in metalloproteolytic activity and promoted the dissemination of glioma cells in the rat 9L glioma model *in vivo* (Figs. 5 and 6). Somewhat surprisingly, the irradiation-induced changes in MMP-2 and TIMP-2 expression were rather enduring, still detectable at 3 weeks after irradiation. We thus propose that not only irradiation of preimplanted tumor cells but also therapeutic irradiation may enhance the invasive behavior of malignant glioma cells. Furthermore, it is tempting to speculate that therapeutic involved-field irradiation might also create a permissive environment for invading glioma cells in the adjacent, non-tumor-bearing brain.

What are the major clinical implications of the present study?

(*a*) Alterations in the fractionation of radiotherapy for human glioblastoma multiforme might be considered. If radiotherapy was initiated with higher single fractions, without increasing the total biological dose to the tumor-bearing brain tissue, cells driven into migration and invasion might be more likely to undergo clonogenic cell death.

(*b*) Inhibitors of migration and invasion, such as marimastat or BAY 12-9566, although of modest antiglioma activity when administered alone, may prevent irradiation-induced dissemination of glioma cells from the target volume of irradiation when administered during radiotherapy.

(*c*) Future studies will have to determine whether the biological effects of irradiation identified in glioma cells can be reproduced in other cancer cell types, thus broadening the significance of the data reported here.

ACKNOWLEDGMENTS

We thank C. Grimmel, S. Haid, and G. von Kuerthy for excellent technical support.

REFERENCES

1. Fine, H., Dear, K., Loeffler, J., Black, P., and Canellos, G. Meta-analysis of radiation therapy with and without adjuvant chemotherapy for malignant gliomas in adults. Cancer (Phila.), *71:* 2585–2597, 1993.
2. Hochberg, F., and Pruitt, A. Assumptions in the radiotherapy of glioblastomas. Neurology, *30:* 907–911, 1980.
3. Mornex, F., Nayel, H., and Taillandier, L. Radiation therapy for malignant astrocytomas in adults. Radiother. Oncol., *27:* 181–192, 1993.
4. Garden, A., Maor, M. H., Yung, W. K., Bruner, J. M., Woo, S. Y., Moser, R. P., and Lee, Y. Y. Outcomes and patterns of failure following limited-volume irradiation for malignant astrocytomas. Radiother. Oncol., *20:* 99–110, 1991.
5. Hess, C., Schaaf, J., Kortmann, R., Schabet, M., and Bamberg, M. Malignant glioma: patterns of failure following individually tailored limited volume irradiation. Radiother. Oncol., *30:* 146–149, 1994.
6. Massey, V., and Wallner, K. Patterns of second recurrence of malignant astrocytomas. Int. J. Radiat. Oncol. Biol. Phys., *18:* 395–398, 1990.
7. Sethi, T., Rintoul, R. C., Moore, S. M., MacKinnon, A. C., Salter, D., Choo, C., Chilvers, E. R., Dransfield, I., Donnelly, S. C., Strieter, R., *et al.* Extracellular matrix proteins protect small lung cancer cells against apoptosis: a mechanism for small lung cancer growth and drug resistance *in vivo*. Nat. Med., *5:* 662–668, 1999.
8. Platten, M., Wick, W., Wild-Bode, C., Aulwurm, S., Dichgans, J., and Weller, M. Transforming growth factors β1 (TGF-β_1) and TGF-β_2 promote glioma cell migration via up-regulation of $\alpha_V\beta_3$ integrin expression. Biochem. Biophys. Res. Commun., *268:* 607–611, 2000.
9. Pijuan-Thompson, V., and Gladson, C. Ligation of integrin $\alpha_5\beta_1$ is required for internalization of vitronectin by integrin $\alpha_V\beta_3$. J. Biol. Chem., *272:* 2736–2743, 1997.
10. Brooks, P. C., Strömblad, S., Sanders, L. C., von Schalscha, T. L., Aimes, R. T., Stetler-Stevenson, W. G., Quigley, J. P., and Cheresh, D. A. Localization of matrix metalloproteinase MMP-2 to the surface of invasive cells by interaction with integrin $\alpha_V\beta_3$. Cell, *85:* 683–693, 1996.
11. Amberger, V., Hensel, T., Ogata, N., and Schwab, M. Spreading and migration of human glioma and rat C6 cells on central nervous system myelin *in vitro* is correlated with tumor malignancy and involves a metalloproteolytic activity. Cancer Res., *58:* 149–158, 1998.
12. Bian, J., and Sun, Y. Transcriptional activation by p53 of the human type IV collagenase (gelatinase A or matrix metalloproteinase 2) promoter. Mol. Cell. Biol., *17:* 6330–6338, 1997.
13. Reed, J. Double identity for proteins of the Bcl-2 family. Nature (Lond.), *387:* 773–776, 1997.
14. Zhang, Z., Vuori, K., Wang, H-G., Reed, J., and Ruoslahti, E. Integrin activation by R-ras. Cell, *85:* 61–69, 1996.
15. Wick, W., Wagner, S., Kerkau, S., Dichgans, J., Tonn, J. C., and Weller, M. BCL-2 promotes migration and invasiveness of human glioma cells. FEBS Lett., *440:* 419–424, 1998.
16. Roth, W., Fontana, A., Trepel, M., Dichgans, J., Reed, J. C., and Weller, M. Immunochemotherapy of malignant glioma: synergistic activity of CD95 ligand and chemotherapeutics. Cancer Immunol. Immunother., *44:* 55–63, 1997.
17. Bartussek, C., Naumann, U., and Weller, M. Accumulation of mutant p53(V143A) modulates the growth, clonogenicity, and radiochemosensitivity of malignant glioma cells independent of endogenous p53 status. Exp. Cell Res., *253:* 432–439, 1999.
18. McDonald, A. C., and Brown, R. Induction of p53-dependent and p53-independent cellular responses by topoisomerase 1 inhibitors. Br. J. Cancer, *78:* 745–751, 1998.
19. Wierzbicka-Patynowski, I., Niewiarowski, S., Marcinkiewicz, C., Calvete, J. J., Marcinkiewicz, M. M., and McLane, M. A. Structural requirements of echistatin for the recognition of $\alpha_V\beta_3$ and $\alpha_5\beta_1$ integrins. J. Biol. Chem., *274:* 37809–37814, 1999.
20. Loeffler, J., Alexander, E., III, Hochberg, F. H., Wen, P. Y., Morris, J. H., Schoene, W. C., Siddon, R. L., Morse, R. H., and Black, P. M. Clinical patterns of failure following stereotactic interstitial irradiation for malignant gliomas. Int. J. Radiat. Oncol. Biol. Phys., *19:* 1455–1462, 1999.
21. Weller, M., Malipiero, U., Aguzzi, A., Reed, J. C., and Fontana, A. Protooncogene *bcl-2* gene transfer abrogates Fas/APO-1 antibody-mediated apoptosis of human malignant glioma cells and confers resistance to chemotherapeutic drugs and therapeutic irradiation. J. Clin. Investig., *95:* 2633–2643, 1995.
22. Strik, H., Deininger, M., Streffer, J., Grote, E., Wickboldt, J., Dichgans, J., Weller, M., and Meyermann, R. BCL-2 family protein expression in initial and recurrent glioblastomas: modulation by radiochemotherapy. J. Neurol. Neurosurg. Psychiatry, *67:* 763–768, 1999.
23. Van Meir, E. G., Kikuchi, T., Tada, M., Li, H. Diserens, A. C., Wojcik, B. E., Huang, H. J. S., Freimann, T., de Tribolet, N., and Cavenee, W. K. Analysis of the *p53* gene and its expression in human glioblastoma cells. Cancer Res., *54:* 649–652, 1994.
24. Weller, M., Rieger, J., Grimmel, C., van Meir, E. G., de Tribolet, N., Krajewski, S. Reed, J. C., von Deimling, A., and Dichgans, J. Predicting chemoresistance in human malignant glioma cells: the role of molecular genetic analysis. Int. J. Cancer, *79:* 640–644, 1998.
25. Albini, A., Iwamoto, Y., Kleinman, H. K., Martin, G. R., Aaronson, S. A., Kozlowski, J. M., and McEvan, R. M. A rapid *in vitro* assay for quantitating the invasive potential of tumor cells. Cancer Res., *47:* 3239–3245, 1987.
26. Pedersen, P., Marienhagen, K., Mork, S., and Bjerkvig, R. Migratory pattern of fetal rat brain cells and human glioma cells in the adult rat brain. Cancer Res., *53:* 5158–5165, 1993.
27. Dahlstrand, J., Collins, V., and Lendahl, U. Expression of the class VI intermediate filament nestin in human central nervous system tumors. Cancer Res., *52:* 5334–5341, 1992.
28. Zhang, H., Kelly, G., Zerillo, C. Jaworski, D. M., and Hockfield, S. Expression of a cleaved brain-specific extracellular matrix protein mediates glioma cell invasion *in vivo*. J. Neurosci., *18:* 2370–2376, 1998.

Sublethal Irradiation Promotes Migration and Invasiveness of Glioma Cells: Implications for Radiotherapy of Human Glioblastoma

Christine Wild-Bode, Michael Weller, Andreas Rimner, et al.

Cancer Res 2001;61:2744-2750.